Korean J. Chem. Eng., 32(11), 2264-2272 (2015)
DOI: 10.1007/s11814-015-0045-7

pISSN: 0256-1115
eISSN: 1975-7220

Effect of solution properties on the interaction of ^{90}Sr(II) with GMZ bentonite

Xin Chen*, Jin Wang*, Shaowei Wang, Fengliang Ma***, Xiaopeng Chen*, and Jiaxing Li****,†**

*School of Resources & Environmental Engineering, Hefei University of Technology, No. 193 Tunxi Road, Hefei 230009, Anhui Province, China
**Nuclear and Radiation Safety Center, Ministry of Environment Protection of the People's Republic of China, Beijing 100082, China
***Research Institute of Petroleum Exploration & Development-Northwest, Petrochina, Lanzhou, China
****Collaborative Innovation Center of Radiation Medicine of Jiangsu Higher Education Institutions, P. R. China
(*Received 3 December 2014 • accepted 25 February 2015*)

Abstract−The bentonite from gaomiaozi county (Inner Mongolia, China) (GMZ bentonite) has been selected as the candidate of backfill material in China for nuclear waste repository. Herein, the sorption of ^{90}Sr(II) on GMZ bentonite was investigated as a function of contact time, solid content, pH, ionic strength, foreign ions, humic acid (HA) and temperature. The results indicated that the sorption of ^{90}Sr(II) was mainly dominated by ion exchange or outer-sphere surface complexation at low pH, whereas inner-sphere surface complexation was the main sorption mechanism at high pH values. The thermodynamic parameters (ΔH^0, ΔS^0 and ΔG^0) calculated from the temperature-dependent sorption isotherms indicated that the sorption of ^{90}Sr(II) on GMZ bentonite was an endothermic and spontaneous process. The results provided important information for the interaction mechanism of ^{90}Sr(II) with GMZ bentonite, and is crucial for the evaluation of GMZ bentonite as backfill material.

Keywords: GMZ Bentonite, ^{90}Sr(II), Sorption, Kinetic, Thermodynamic Data

INTRODUCTION

With the development of nuclear energy and various nuclear reaction processes, a large amount of radionuclides is released into natural environment. The transport of radionuclides in the natural environment is generally dominated by sorption reactions, colloid formation, complexation, etc. [1-3]. These interactions at water-solid interface are affected by many factors, such as solution pH, ionic strength, the temperature, surface properties of solid, the nature of metal ions and the nature of solid in the system [4,5]. The understanding of the migration behavior of radionuclides is essential for a suitable long-term safety assessment of potential nuclear waste disposal sites, and of substance dumps and sites with radioactive and/or heavy metal ions containing inventory [6].

Bentonite, one of the most common alumino-silicate clay minerals, is considered as a main candidate in the decontamination and treatment of detrimental metal ions because of its low permeability, low cost and high sorption capacity for organic and inorganic pollutants [7-9]. The sorption of radionuclides on bentonite has been studied extensively in the last decade [10,11]. The results indicated that the sorption of radionuclides increased with increasing pH, and the sorption was mainly dominated by outer-sphere surface complexation or ion-exchange at low pH values but by inner-sphere surface complexation or surface precipitation at high pH values [12-14]. In China, the bentonite in Gaomiaozi county (Inner Mongolia, China) (herein named as GMZ bentonite) has been selected as the candidate of backfill material for nuclear waste repository [15,16]. Previous studies reported that GMZ bentonite was a suitable material in the preconcentration and solidification of heavy metal ions from large volume of aqueous solutions [17,18]. The results revealed that the GMZ bentonite had high sorption capacity in the removal of radionuclides from aqueous solutions and it could be used as backfill material. However, according to our literature survey, few studies were focused on the sorption of ^{90}Sr(II) on GMZ bentonite as affected by humic acid and coexisting electrolyte ions. ^{90}Sr(II) is the main radionuclide in the spent fuel. Hence, the interaction of ^{90}Sr(II) with GMZ bentonite should be investigated intensively because radiostronium is considered as one of the most hazardous radionuclides among the fission byproducts for human health due to its long half-life [19].

The basic objectives of this paper are: (1) to study the effect of different environmental parameters on ^{90}Sr(II) sorption, such as pH, ionic strength, solid content, foreign ions, humic acid and temperature by using batch technique; (2) to investigate the sorption kinetics and to calculate the thermodynamics parameters of ^{90}Sr(II) sorption on GMZ bentonite; (3) to presume the sorption mechanism of ^{90}Sr(II) on GMZ bentonite and to estimate the possible application of GMZ bentonite in nuclear waste disposal.

EXPERIMENTAL

1. Materials

The GMZ bentonite was obtained from Gaomiaozi County (Inner Mongolia, China). It was converted into Na-bentonite by treating with 1.0 M NaCl, then washing with doubly distilled water until it was free of chloride ions. Then the sample was dried and ground

†To whom correspondence should be addressed.
E-mail: lijx@ipp.ac.cn

to pass 53 μm sieve. The main components of the sample were: SiO_2 60.58%, Na_2O 1.42%, MgO 1.86%, CaO 0.98%, Al_2O_3 1.92%, Fe_2O_3 4.00%, K_2O 0.75%, MnO 0.05% [20]. The water content of 5.7% was taken into account in the calculation of the Na-bentonite content. In the following sections, we call the GMZ Na-bentonite simply as GMZ bentonite.

Humic acid (HA) was extracted from the soil samples of Hua-Jia ridge of Gansu province near 35 °N and 105 °E, which is very near to the site of nuclear weapon tests and also very near to the site of a nuclear waste repository. It has been characterized in detail [21,22]. The main elements of HA are: C 60.44%, H 3.53%, N 4.22%, O 31.31% and S 0.50%.

The stock solution of ^{90}Sr(II) was prepared by dissolving weighed amounts of $Sr(NO_3)_2$. It was performed by mixing 21.74 mg $Sr(NO_3)_2$ and 500 mL Milli-Q water under ambient temperature and the concentration of ^{90}Sr(II) solution was 18mg/L. The radionuclide ^{90}Sr(II) was used as radiotracer in the experiments.

All reagents with analytical reagent grade were purchased from Sinopharm Chemical Reagent Co., Ltd. and used as received without any further purification. Milli-Q water was used in all experiments.

2. Characterization

The X-ray powder diffraction (XRD) pattern of the GMZ bentonite crystal was recorded on a MAC Science Co. M18XHF diffractometer. XRD analysis was performed with CuKα radiation (λ=0.15406 nm) with a Rigaku X-ray diffractometer. The 2θ-scanning rate was 2 min^{-1}. Patterns were identified by comparison to the JCPD standards.

The sample of GMZ bentonite was also characterized using Fourier transform infrared spectroscopy (FTIR) (Perkin Elmer spectrum 100, America) in pressed KBr pellets. The spectral resolution was set to 1 cm^{-1}, and 150 scans were collected for each spectrum.

3. Sorption Procedures

The sorption of ^{90}Sr(II) on GMZ bentonite was investigated by batch technique in polyethylene tubes sealed with screw-cap under ambient conditions. A stock suspension of GMZ bentonite, stock solutions of electrolyte, ^{90}Sr(II), and HA were added into the test tubes to achieve the desired concentrations of different components and to maintain total volume of 6 mL. Then the pH values were achieved to the desired values by adding negligible volume of 0.1 or 0.01 mol/L HNO_3 or NaOH solutions. After the suspension was shaken for 24 h, the solid phase was separated by centrifugation at 9,000 rpm for 15 min, which was enough to separate the solid phase from liquid phase. The results of blank experiments indicated that the sorption of ^{90}Sr(II) on tube walls was negligible.

The concentration of ^{90}Sr(II) in supernatant was analyzed by liquid scintillation counting (Packard 3100 TR/AB Liquid Scintillation analyzer, Perkin-Elmer) with the scintillation cocktail (ULTIMA GOLD AB^{TM}, Packard). The amount of ^{90}Sr(II) adsorbed on GMZ bentonite was calculated from the difference between the initial concentration (C_0) and the equilibrium one (C_e). The sorption of ^{90}Sr(II) and the distribution coefficient (K_d) were calculated from the following equation:

$$\text{Sorption}\% = \frac{C_0 - C_e}{C_0} \times 100 \quad (1)$$

$$K_d = \frac{C_0 - C_e}{C_e} \times \frac{V}{m} \quad (2)$$

where C_0 (mg/L) is the initial concentration, C_e (mg/L) is the equilibrium concentration, m (g) is the mass of GMZ bentonite, and V (L) is the volume of suspension.

All the experimental data were the average of duplicate experiments and the relative errors of data were less than 5%.

RESULTS AND DISCUSSION

1. XRD and FTIR Characterization

The XRD pattern of GMZ bentonite is given in Fig. 1. The characteristic diffraction peaks of the plane at 2θ values of 19.92°, 35.0° and 63.0° indicate that the main compound is montmorillonite (M) and the corresponding basal spacing of 4.45 Å further implies the 2 : 1 mineral type. The peaks at 26.3° and 28.1° represent the

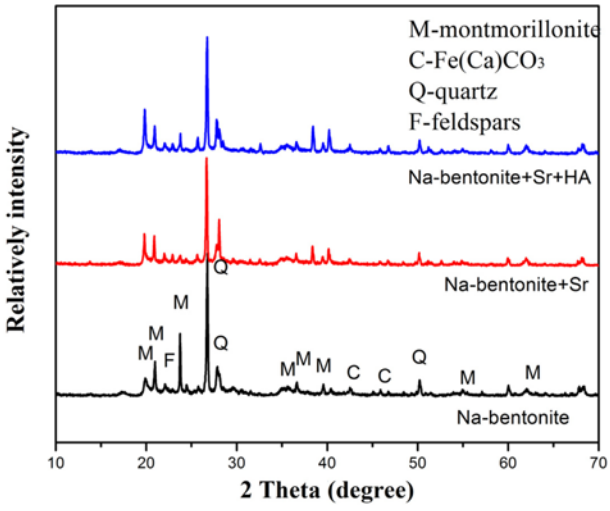

Fig. 1. The XRD pattern of Na-bentonite; Na-bentonite+Sr; Na-bentonite+Sr+HA.

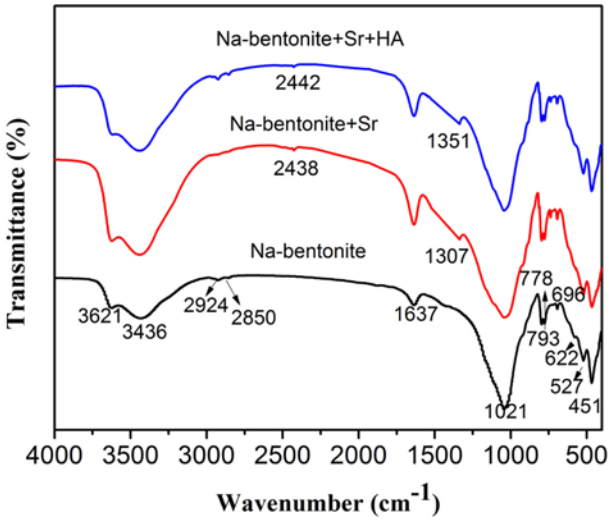

Fig. 2. The FT-IR spectrum of Na-bentonite; Na-bentonite+Sr; Na-bentonite+Sr+HA.

presence of quartz as impurity. The XRD pattern also indicates the presence of calcite (C: 42.4°) and feldspar (F: 22.3°) [23]. From Fig. 1, one can also see the crystallinity of GMZ bentonite after ^{90}Sr(II) sorption is very close to that of sample before sorption, indicating that the structure of GMZ bentonite almost remains intact and cannot be damaged after sorption process.

Fig. 2 shows the FTIR spectrum of GMZ bentonite. The absorption band at 3,621 cm^{-1} is due to the stretching vibration of structural OH group. Water in GMZ bentonite gives a broad band at 3,436 cm^{-1} corresponding to the H_2O-stretching vibrations, due to an overtone of the bending vibration of water observed at 1,637 cm^{-1}. The bands at 2,924 and 2,850 cm^{-1} are due to the aliphatic C-H stretching vibration. The very strong band at 1,021 cm^{-1} is due to Si-O bending vibrations. A sharp stretching vibration band at 793 cm^{-1} with inflexion near 778 cm^{-1} confirms the quartz admixture in the sample. The stretching vibration band at 696 cm^{-1} is due to the deformation and bending modes of the Si-O bond. The band at 622 cm^{-1} is assigned to coupled Al-O and Si-O out-of-plane vibrations. The bands at 527 and 451 cm^{-1} are due to Al-O-Si and Si-O-Si bending vibrations, respectively. Note that the peak at 2,438, 2,442, 1,351 and 1,307 cm^{-1} could be attributed to the dispurities of sample after ^{90}Sr(II) sorption [24]. Besides, no obvious changes of spectral band intensities, shapes, and positions are observed after ^{90}Sr(II) and HA sorption on Na-bentonite surfaces. The presence of HA may change the spectral band in the spectroscopic analysis, but its lower concentration leads to the signal being indiscernible.

2. Effect of Contact Time

The sorption of ^{90}Sr(II) on GMZ bentonite at pH 6.0 as a function of contact time is shown in Fig. 3. The sorption of ^{90}Sr(II) on GMZ bentonite increased rapidly during the first contact time of 7 h and then the sorption was maintained a high level with increasing contact time. The result indicates that ^{90}Sr(II) sorption on GMZ bentonite is mainly attributed to chemical sorption rather than physical sorption [25]. In the following experiments, 12 h was selected to achieve the sorption equilibration.

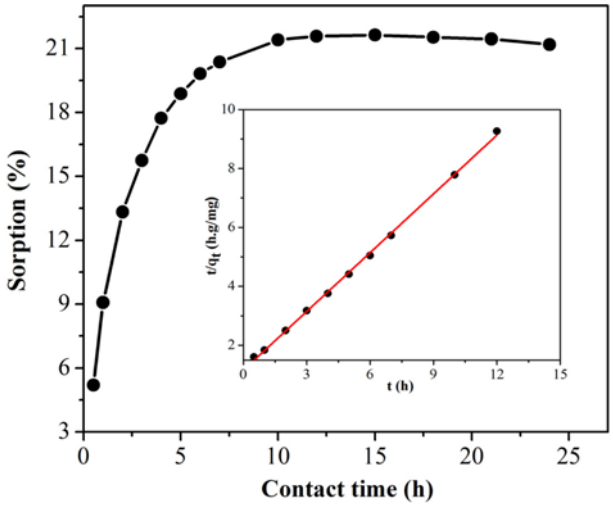

Fig. 3. Effect of contact time on ^{90}Sr(II) sorption onto GMZ Na-bentonite, $C_{[Sr(II)]initial}$=3 mg/L, m/V=0.5 g/L, I=0.01 M $NaNO_3$, pH=6.0±0.1, T=298 K.

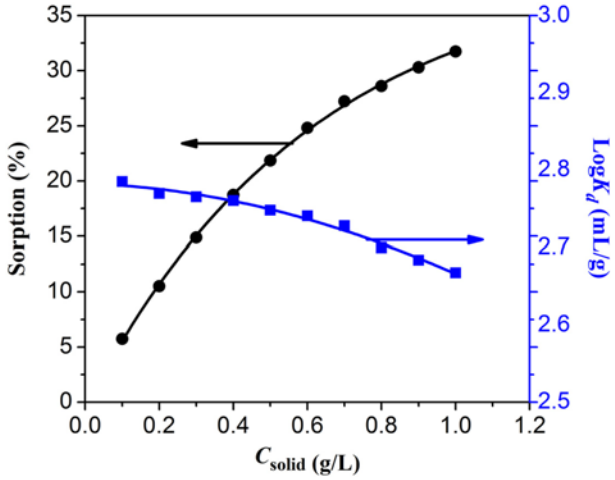

Fig. 4. Effect of solid content on ^{90}Sr(II) sorption onto GMZ Na-bentonite, $C_{[Sr(II)]initial}$=3 mg/L, I=0.01 M $NaNO_3$, pH=6.0±0.1, t=24 h, T=298 K.

A pseudo-second-order rate equation is used to simulate the kinetic sorption [26]:

$$\frac{t}{q_t} = \frac{1}{2kq_e^2} + \frac{1}{q_e}t \quad (3)$$

where k (g/(mg·h)) is the pseudo-second-order rate constant of sorption, q_t (mg/g of dry mass) is the amount of ^{90}Sr(II) adsorbed on the surface of the adsorbent at time t (h), and q_e (mg/g of dry mass) is the equilibrium sorption capacity. A linear of t/q_t vs. t is achieved (Fig. 3). The k and q_e values calculated from the slope and intercept are 0.332 g·$mg^{-1}h^{-1}$ and 1.5049 mg/g, respectively. The correlation coefficient of the pseudo-second-order rate equation for the linear plot is 0.999, suggesting that the kinetic sorption can be described by the pseudo-second-order rate model well.

3. Effect of Solid Content

The sorption of ^{90}Sr(II) on GMZ bentonite as a function of solid content is shown in Fig. 4. The result demonstrates that the removal of ^{90}Sr(II) from solution to GMZ bentonite increases with increasing solid content. With increasing solid content, the amount of functional groups at GMZ bentonite surface increases, and thereby more groups are available to bind ^{90}Sr(II). However, one can see that the K_d value decreases a little with increasing solid content. The physicochemical property of K_d value is independent of solid content at low content. The decrease of K_d value with increasing solid content may be attributed to the competition among the functional groups at the surface of GMZ bentonite. Such competition reduces the available sites of functional groups, and thereby results in the decreasing of sorption ability of GMZ bentonite with increasing solid content [17].

4. Effect of pH

The pH value is an important parameter that influences the sorption of metal ions on the solid particles. The effect of pH on ^{90}Sr(II) sorption to GMZ bentonite is presented in Fig. 5 and the results indicate that the sorption of ^{90}Sr(II) is strongly dependent on pH. The sorption of ^{90}Sr(II) on GMZ bentonite increased slowly at pH ranging from 3.0 to 6.0, then increased drastically from pH 6.0 to

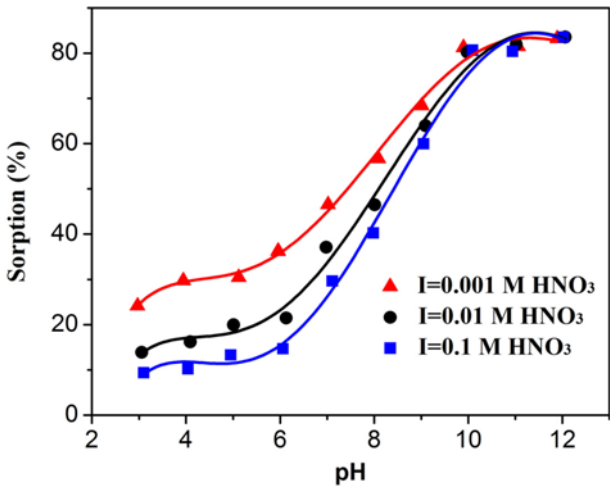

Fig. 5. Effect of pH and ionic strength on ^{90}Sr(II) sorption onto GMZ Na-bentonite, $C_{[Sr(II)]initial}$=3 mg/L, m/V=0.5 g/L, t=24 h, T=298 K.

10.0, and finally maintained the high level at pH>10.0.

The pH-dependence of ^{90}Sr(II) sorption can be attributed to two factors: (1) the surface properties of GMZ bentonite; (2) the species of ^{90}Sr(II) in aqueous solution at different pH values.

The increase of ^{90}Sr(II) sorption on GMZ bentonite with increasing solution pH can be attributed to the surface properties of GMZ bentonite in terms of surface charge and dissociation of functional groups [27]. Since the surface of GMZ bentonite contains two types of sites, ≡SNa/≡SH (ion exchange site) and ≡SOH (surface complexation site), the surface groups of GMZ bentonite can be protonated in two different ways in aqueous system [28]. (1) The surface of GMZ bentonite is positively charged at low pH due to the protonation reaction on the surface ($\equiv SOH+H^+ \leftrightarrow SOH_2^+$). The low sorption efficiency is attributed to the electrostatic repulsion between metal ions (Sr^{2+} is the major species of ^{90}Sr(II) in the solution at the experimental pH) and the edge groups with positive charge ($\equiv SOH_2^+$) on the surface of GMZ bentonite [29]. Besides, the sorption of ^{90}Sr(II) on GMZ bentonite in this pH range can proceed via ion exchange with hydrogen and sodium ions that saturate the exchange sites ($2\equiv SH+Sr^{2+} \rightarrow \equiv S_2\text{-}Sr+2H^+$ or $2\equiv SNa+Sr^{2+} \rightarrow \equiv S_2\text{-}Sr+2Na^+$); (2) At high pH values, the surface of GMZ bentonite becomes negatively charged due to the deprotonation reaction ($\equiv SOH \leftrightarrow \equiv SO^- + H^+$) [30] and electrostatic repulsion decreases with raising pH due to the reduction of positive charge density on the sorption edges, which enhances the sorption of positively charged ^{90}Sr(II) ions through electrostatic force of attraction. Moreover, more surface functional groups are dissociated at high pH values, which provides more available sorption sites and therefore causes higher ^{90}Sr(II) sorption.

According to ^{90}Sr(II) hydrolysis constants, $\log\beta_1$=−13.29 and $\log\beta_2$=−28.51 [31], the species of Sr^{2+} are present at a significant concentration in the studied pH range from 3.0 to 12.0, and the $Sr(OH)^+$ species is negligible between pH 3.0 and 12.0. Thereby, it is almost impossible to form $Sr(OH)_2$ precipitation at the whole experimental pH range. Since there are a great number of functional groups present on the external surfaces of GMZ bentonite, the ion exchange and surface complexation may be the main interaction mechanism of ^{90}Sr(II) sorption on GMZ bentonite [32,33]. The process can be expressed as follows [34]:

(1) to exchange with hydronium ions:

$$2\equiv S\text{-}OH+Sr^{2+} \rightarrow (\equiv S\text{-}O)_2\text{-}Sr=2H^+ \quad (4)$$

$$2\equiv SH+Sr^{2+} \rightarrow S_2\text{-}Sr+2H^+ \quad (5)$$

(2) to exchange with Na^+ ions:

$$2\equiv S\text{-}ONa+Sr^{2+} \rightarrow (\equiv S\text{-}O)_2\text{-}Sr+2Na^+ \quad (6)$$

$$2\equiv SNa+Sr^{2+} \rightarrow \equiv S_2\text{-}Sr+2Na^+ \quad (7)$$

(3) to form complexes with hydrolyzed species:

$$\equiv S\text{-}ONa+H_2O+Sr^{2+} \rightarrow \equiv S\text{-}OSrOH+Na^+ + H^+ \quad (8)$$

The effect of pH on the sorption of ^{90}Sr(II) to GMZ bentonite is the result of the combination of these factors as mentioned above. Similar results of ^{90}Sr(II) sorption on other clay minerals were also reported [35,36].

5. Effect of Ionic Strength

Effect of ionic strength on ^{90}Sr(II) sorption on GMZ bentonite as a function of pH is also shown in Fig. 5. As illustrated in Fig. 5, the sorption of ^{90}Sr(II) on GMZ bentonite is obviously influenced by ionic strength at pH<10.0, and no obvious influence is found at pH>10.0.

The influence of $NaNO_3$ concentration on ^{90}Sr(II) sorption is mainly due to the competition of Na^+ with ^{90}Sr(II) on GMZ bentonite surfaces. The pH- and ionic strength-dependent sorption of ^{90}Sr(II) suggests that the sorption of ^{90}Sr(II) on GMZ bentonite is dominated by ion exchange or outer-sphere surface complexion at low pH, whereas the sorption is mainly due to inner-sphere complexion at high pH [37,38].

To explain the variation and relationship of pH, C_e (mol/L, the concentration of ^{90}Sr(II) remained in solution), and C_s (mol/g, the concentration of ^{90}Sr(II) adsorbed on solid phase), the experimental data of ^{90}Sr(II) sorption in 0.1, 0.01 and 0.001 M $NaNO_3$ are plotted as three-dimensional plots of C_s, C_e and pH (Fig. 6). On the pH-C_s plane, one can see that sorption of ^{90}Sr(II) on GMZ bentonite is strongly dependent on pH values, which is quite similar to the results shown in Fig. 5. On the pH-C_e plane, the concentration

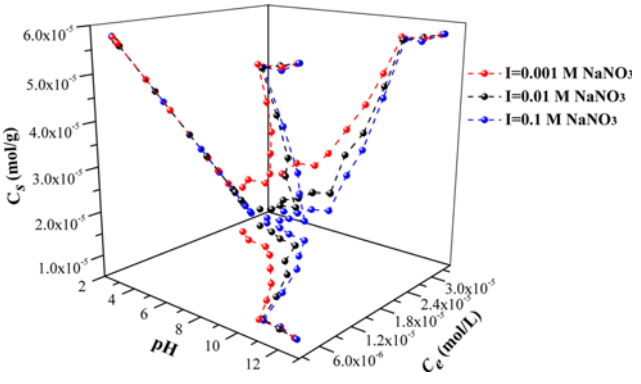

Fig. 6. 3-D plots of ^{90}Sr(II) sorption onto GMZ Na-bentonite as a function of pH and ionic strength, $C_{[Sr(II)]initial}$=3 mg/L, m/V=0.5 g/L, t=24 h, T=298 K.

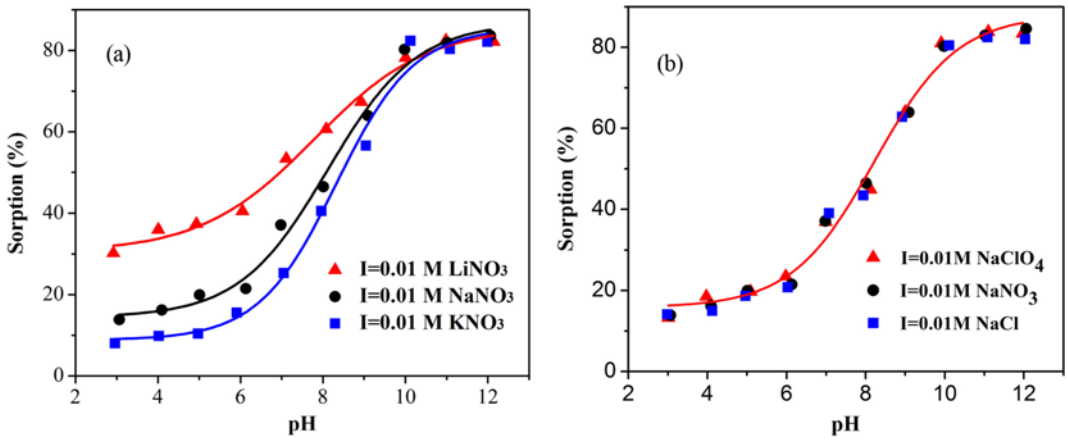

Fig. 7. Effect of pH and foreign cation ions (a) and anion ions (b) on the sorption of ^{90}Sr(II) on GMZ Na-bentonite, $C_{[Sr(II)]initial}$=3 mg/L, m/V=0.5 g/L, t=24 h, T=298 K.

of ^{90}Sr(II) remained in solution decreases with increasing pH at pH 3.0-10.0, and then maintains a low level within pH 10.0-12.0. The projection on the pH-C_e plane is just the inverted image of the projection on the pH-C_s plane. On the C_e-C_s plane, all experimental data in the projection lie in a straight line. The following equation can describe the relationship of C_e-C_s:

$$VC_0 = mC_s + VC_e \quad (9)$$

$$C_s = C_0\frac{V}{m} - C_e\frac{V}{m} \quad (10)$$

where V is the volume and m is the mass of Na-bentonite. The slope (−V/m) and the intercept (C_0·V/m) calculated from C_e-C_s line are −2 and 7×10^{-5}, quite in agreement with the values of m/V=0.5 (g/L) and $C_0=3.42\times10^{-5}$ (mol/L). The three-dimensional plots show the relationship of pH, C_e, and C_s very clearly: all the data of C_e-C_s lies in a straight line with slope (−V/m) and intercept (C_0·V/m) at same initial ^{90}Sr(II) concentration and same adsorbent content.

6. Effect of Foreign Ions

To investigate the effect of foreign cation on the sorption of ^{90}Sr(II), the sorption of ^{90}Sr(II) on GMZ bentonite was investigated in 0.01 M $LiNO_3$, $NaNO_3$ and KNO_3 solutions, respectively (Fig. 7(a)). The sorption of ^{90}Sr(II) on GMZ bentonite is obviously influenced by the cation ions in the suspension. At pH<10.0, the sorption percentages of ^{90}Sr(II) on GMZ bentonite under the same pH values are in the following sequences of Li^+>Na^+>K^+, indicating that the cation ions can alter the surface properties of GMZ bentonite [39]. The sorption of ^{90}Sr(II) on GMZ bentonite can be considered as a competition of ^{90}Sr(II) with Li^+ (or Na^+, K^+) at GMZ bentonite surfaces. The hydration radius of the three cation ions is K^+=2.32 Å, Na^+=2.76 Å and Li^+=3.4 Å [40]. The hydration ratio of K^+ is smaller than that of the other two cation ions, and therefore the influence of K^+ on ^{90}Sr(II) sorption is more obvious than that of Na^+ and Li^+. In general, the influence of monovalent alkali ions on the sorption of bivalent ^{90}Sr(II) should be weak. However, at pH 3-10, the influence of Li^+, Na^+ and K^+ on ^{90}Sr(II) sorption is drastic. Before the addition of ^{90}Sr(II) ions, the GMZ bentonite has been pre-equilibrated with the alkali ions. The sorption of ^{90}Sr(II) on GMZ bentonite can be considered as the exchange of ^{90}Sr(II) with alkali ions and other reactions [41]. Thereby, it is reasonable that the alkali ions can affect ^{90}Sr(II) sorption obviously.

Fig. 7(b) shows the effect of foreign anion ions on the sorption of ^{90}Sr(II) from aqueous solution to GMZ bentonite in 0.01 M $NaClO_4$, $NaNO_3$ and NaCl solutions, respectively. From Fig. 7(b), one can see that the sorption of ^{90}Sr(II) on GMZ bentonite is not influenced by the background electrolyte foreign anion ions. The radius order of inorganic acid radicals is Cl^-<NO_3^-<ClO_4^-. Such negatively charged anions may form complexes with the oxygen-containing functional groups on the GMZ bentonite surfaces. However, the effects of Cl^-, NO_3^- and ClO_4^- on ^{90}Sr(II) sorption to GMZ bentonite are still very weak, suggesting that surface complexes are formed on surfaces of GMZ bentonite. The effect of foreign anion ions on ^{90}Sr(II) removal from aqueous solution to GMZ bentonite can be negligible. The results are consistent with the sorption of Ni(II) on GMZ bentonite [20]. However, Tan et al. [42] reported that the sorption of Co(II) on Na-attapulgite was influenced by foreign anion ions. The results

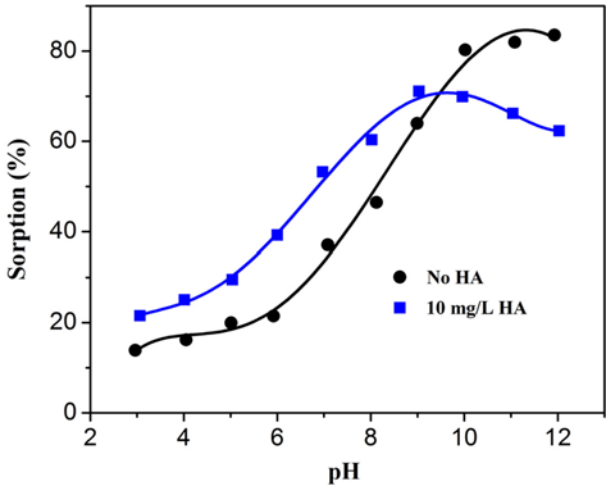

Fig. 8. Effect of HA on ^{90}Sr(II) sorption onto GMZ Na-bentonite, $C_{[Sr(II)]initial}$=3 mg/L, m/V=0.5 g/L, I=0.01 M $NaNO_3$, t=24 h, T=298 K.

indicate that the influence of foreign anion ions on sorption of metal ions is dominated by various factors, such as the properties of metal ions and the surface properties of adsorbent.

7. Effect of HA

The pH dependence of ^{90}Sr(II) sorption on GMZ bentonite in the absence and presence of HA is shown in Fig. 8. The presence of HA enhances the sorption of ^{90}Sr(II) on HA-bentonite hybrids obviously at pH<9.5, whereas a negative effect is observed at pH>9.5.

Humic acid (HA) is widely present in all soils, sediments, and natural waters. It is a chemically heterogeneous compound containing many functional groups, like carboxyl (-COOH), hydroxyl (-OH), amine (-NH_2) and phenol (Ar-OH) [24]. HA has a macromolecular structure, so only a small fraction of the groups of the "adsorbed" HA are free to interact with ^{90}Sr(II) ions [43]. At low pH, the negatively charged HA can be easily adsorbed on the positively charged GMZ bentonite, so the complexation of surface-adsorbed HA and ^{90}Sr(II) results in the enhancement of ^{90}Sr(II) sorption on GMZ bentonite. At high pH, there are more free HA molecules available in solution because of the negatively charged HA molecules are difficult to be adsorbed on the negatively charged surface of GMZ bentonite at high pH values. The free HA molecules that interacted with ^{90}Sr(II) can form soluble HA-Sr complexes [44] and can stabilize ^{90}Sr(II) in solution, resulting in an overall decrease in ^{90}Sr(II) sorption. The fact that fewer HA molecules are adsorbed on GMZ bentonite (i.e., there are more free HA molecules in solution) indicates that ^{90}Sr(II) ions form complexes with surface adsorbed HA on the surfaces of GMZ bentonite. Therefore, ^{90}Sr(II) sorption on GMZ bentonite decreases with pH increasing at high pH values in the presence of HA. The results are in good agreement with the influence of humic substances on metal ion sorption on clay minerals, i.e., the presence of HA enhances metal ion sorption at low pH and decreases metal ion sorption at high pH [45].

8. Effect of Temperature and Thermodynamic Parameters

Temperature is one of the most important parameters that can affect the physicochemical behavior of metal ions in the environment. The sorption isotherms of ^{90}Sr(II) at 298, 318 and 338 K are shown in Fig. 9(a). It is clear that the sorption isotherm is the highest at T=338 K and is the lowest at T=298 K, suggesting that the sorption process of ^{90}Sr(II) on GMZ bentonite is favored at high temperature. To gain a better understanding of the mechanism and to quantify the sorption data, Langmuir, Freundlich and D-R models are used to fit the sorption isotherms and to simulate the experimental data.

The Langmuir isotherm model is used to describe monolayer sorption onto adsorbent surface containing a number of identical sites. The form of Langmuir can be expressed by the following expression [46]:

$$C_s = \frac{bC_{smax}C_e}{1+bC_e} \tag{11}$$

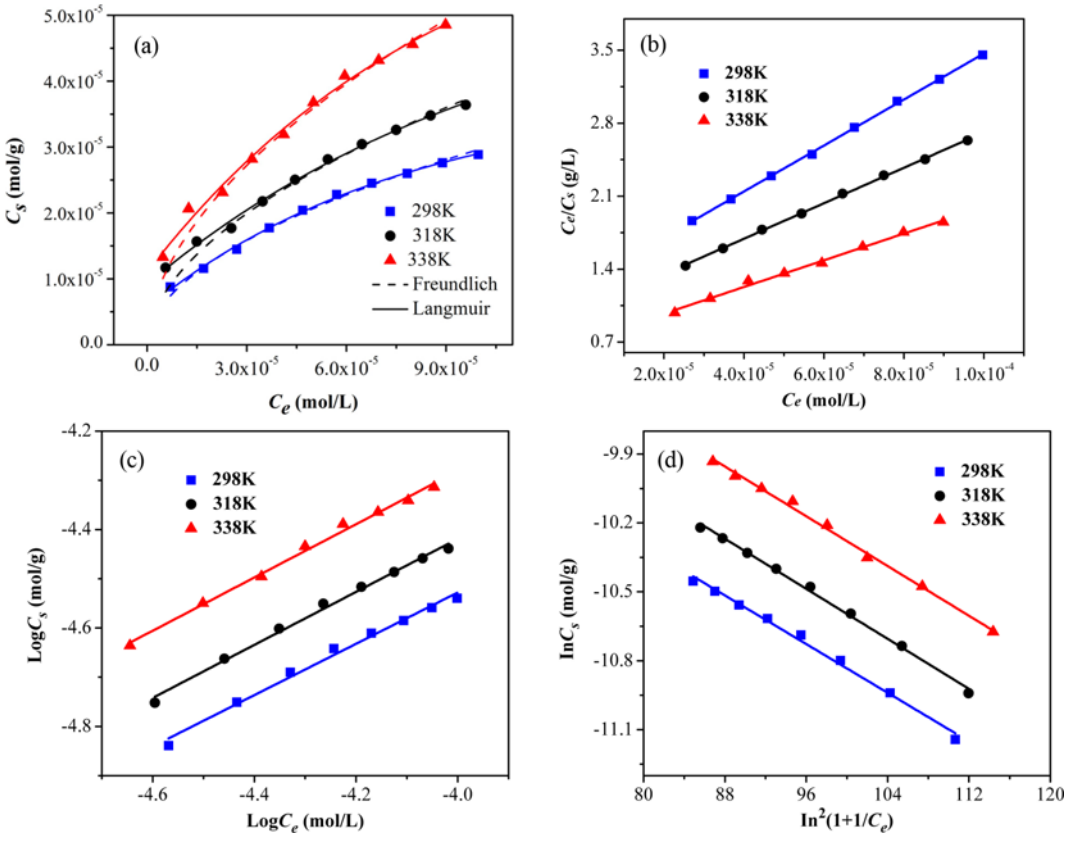

Fig. 9. Sorption isotherms (a) of ^{90}Sr(II) onto GMZ Na-bentonite at three different temperatures, Langmuir (b), Freundlich (c), D-R (d) isotherms of ^{90}Sr(II) sorption onto GMZ Na-bentonite at three different temperatures, m/V=0.5 g/L, I=0.01 M $NaNO_3$, pH=6.0± 0.1, t=24 h.

Eq. (11) can be expressed in the linear form:

$$\frac{C_e}{C_s}=\frac{1}{bC_{smax}}+\frac{C_e}{C_{smax}} \quad (12)$$

where C_e (mol/L) is the equilibrium concentration of $^{90}Sr(II)$ remaining in the solution, the maximum sorption capacity C_{smax} (mol/g) represents the quantity of $^{90}Sr(II)$ adsorbed at complete monolayer coverage, b (L/mol) stands for the Langmuir constant that is related to the sorption heat.

The Freundlich isotherm model represents properly the sorption data at low and intermediate concentrations on heterogeneous surfaces [47]:

$$C_s=k_F C_e^n \quad (13)$$

Eq. (13) can be expressed in linear form:

$$\log C_s=\log k_F+n\log C_e \quad (14)$$

where k_F ($mol^{1-n}L^n/g$) represents the sorption capacity when $^{90}Sr(II)$ equilibrium concentration equals to 1, and n represents the degree of dependence of sorption with equilibrium concentration.

The D-R isotherm model is more general than Freundlich isotherm since it is not limited by the homogeneous surface and constant sorption potential assumption. The D-R equation has the following form [48]:

$$C_s=C_{smax}\exp(-\beta\varepsilon^2) \quad (15)$$

Eq. (15) can be expressed in linear form:

$$\ln C_s=\ln C_{smax}-\beta\varepsilon^2 \quad (16)$$

where C_s and C_{smax} are defined above, b is the activity coefficient related to mean sorption energy (mol^2/kJ^2), and ε is the Polanyi potential, which is equal to:

$$\varepsilon=RT\ln(1+1/C_e) \quad (17)$$

where R is ideal gas constant (8.3145 J/(mol·K)), and T is the absolute temperature in Kelvin (K). E (kJ/mol) is defined as the free energy change, which requires to transfer 1 mol of $^{90}Sr(II)$ from solution to the GMZ bentonite surfaces. The relation is expressed as:

$$E=\frac{1}{\sqrt{2\beta}} \quad (18)$$

The experimental data of $^{90}Sr(II)$ sorption (Fig. 9(a)) are regressively fitted with the Langmuir (Fig. 9B), Freundlich (Fig. 9(c)) and D-R (Fig. 9(d)) isotherm models. The relative values calculated from the three models are listed in Table 1. The correlation coefficients for the Langmuir, Freundlich and D-R isotherms are very close to 1. It can be concluded from R^2 values that the Langmuir model fits the experimental data better than Freundlich and D-R model. The fact that the Langmuir model fits the experimental data well indicates almost complete monolayer coverage of the GMZ bentonite particles. Moreover, the GMZ bentonite has a limited sorption capacity; thus the sorption could be better described by Langmuir model rather than by Freundlich model, as an exponentially increasing sorption was assumed in the Freundlich model. The values of C_{smax} obtained from the Langmuir model for $^{90}Sr(II)$ sorption onto GMZ bentonite are the highest at T=338 K and the lowest at T=298 K, which also indicates that the sorption is enhanced with increasing temperature. In the Freundlich model, the value of n is from unity, which indicates that nonlinear sorption takes place on the heterogeneous surfaces. The magnitude of E is an important factor for estimating the sorption mechanism. The E values obtained from Eq. (18) are 10.76 (298 K), 11.34 (318 K) and 12.07 (338 K) kJ/mol, which are in the sorption energy range of chemical ion-exchange reaction [49,50]. This suggests that $^{90}Sr(II)$ sorption on GMZ bentonite is attributed to chemical sorption rather than physical sorption. The sorption capacities C_{smax} derived from the D-R model are higher than those derived from the Langmuir model. This may be attributed to the different assumptions considered in the formulation of the isotherms.

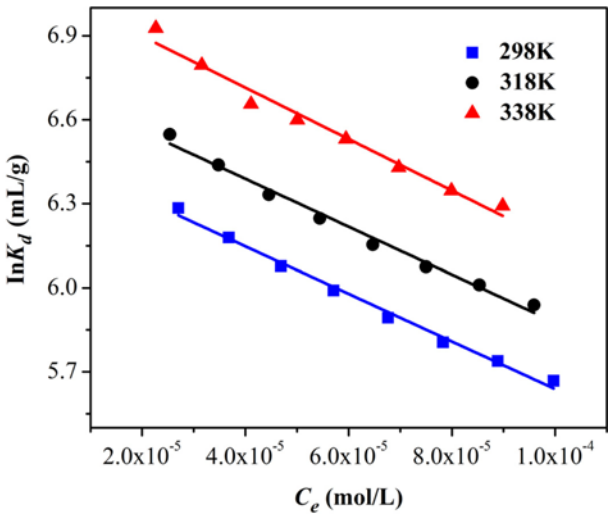

Fig. 10. Linear plots of $\ln K_d$ versus C_e, m/V=0.5 g/L, I=0.01 M $NaNO_3$, pH=6.0±0.1, t=24 h.

The thermodynamic parameters (ΔH^0, ΔS^0 and ΔG^0) for the sorption of $^{90}Sr(II)$ on GMZ bentonite can be calculated from the temperature-dependent sorption isotherms. The value of free energy change (ΔG^0) is calculated from the relationship:

$$\Delta G^0=-RT\ln\Delta K^0 \quad (19)$$

Table 1. Parameters of Langmuir, Freundlich, D-R models for the simulation of $^{90}Sr(II)$ sorption isotherms at different temperatures

T (K)	Langmuir			Freundlich			D-R		
	C_{smax} (mol/g)	B (L/mol)	R^2	k_F ($mol^{1-n}L^n/g$)	n	R^2	B (mol^2/kJ^2)	C_{smax} (mol/g)	R^2
298	4.54×10^{-5}	1.75×10^{4}	0.999	3.61×10^{-3}	0.521	0.981	4.32×10^{-3}	2.79×10^{-4}	0.984
318	5.88×10^{-5}	1.68×10^{4}	0.999	5.44×10^{-3}	0.539	0.975	3.89×10^{-3}	3.81×10^{-4}	0.987
338	7.81×10^{-5}	2.32×10^{4}	0.994	7.60×10^{-3}	0.541	0.982	3.43×10^{-3}	5.15×10^{-4}	0.990

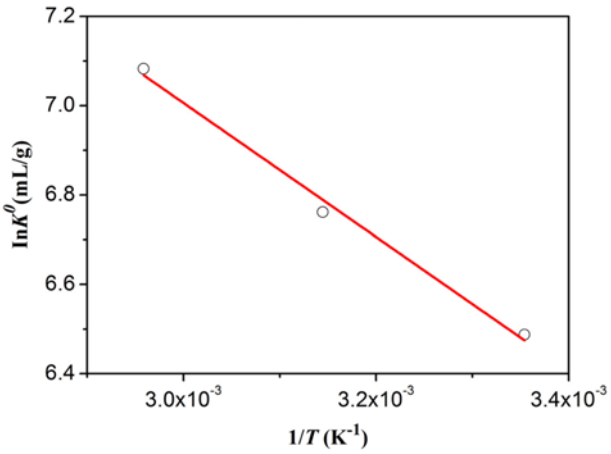

Fig. 11. Linear plot of lnK^0 vs 1/T for the sorption of ^{90}Sr(II) on GMZ Na-bentonite at 298, 318 and 338 K, m/V=0.5 g/L, I=0.01 M $NaNO_3$, pH=6.0±0.1, t=24.

Table 2. Values of thermodynamic parameters for the sorption of ^{90}Sr(II) on GMZ Na-bentonite

T (K)	ΔG^0 (kJ/mol)	ΔS^0 (J/(mol·K))	ΔH^0 (kJ/mol)
298	−16.08		12.47
318	−17.80	95.76	12.66
338	−19.91		12.47

where K^0 is the sorption equilibrium constant. Values of $\ln K^0$ are obtained by plotting $\ln K_d$ versus C_e and extrapolating C_e to zero (Fig. 10). Standard entropy change (ΔS^0) is calculated using the equation:

$$\Delta S^0 = -\left(\frac{\partial \Delta G^0}{\partial T}\right)_p \quad (20)$$

Then the average standard enthalpy change (ΔH^0) is obtained from the equation:

$$\Delta H^0 = \Delta G^0 + T\Delta S^0 \quad (21)$$

Linear plot of $\ln K^0$ versus 1/T for ^{90}Sr(II) sorption on GMZ bentonite is shown in Fig. 11 and the values obtained from Eqs. (19)-(21) are in Table 2. The positive ΔH^0 values indicate that the sorption is endothermic. One possible explanation to this positive ΔH^0 is that ^{90}Sr(II) is solved well in water, and the hydration sheath of ^{90}Sr(II) has to be destroyed before its sorption to GMZ bentonite. This dehydration process needs energy, and it is favored at higher temperature [51,52]. This energy exceeds the exothermicity of ^{90}Sr(II) to attach to the GMZ bentonite surface. This assumption indicates that the endothermicity of the desolvation process is higher than the enthalpy of sorption to a considerable extent. The ΔG^0 values are negative as expected for a spontaneous process under the conditions applied. The value of ΔG^0 becomes more negative with the increase of temperature, which indicates more efficient sorption at high temperature. At high temperature, cations are readily desolvated and hence its sorption becomes more favorable. The positive value of ΔS^0 suggests the affinity of GMZ bentonite toward ^{90}Sr(II) in aqueous solutions and may suggest some structure changes on GMZ bentonite [53]. The ΔS^0 parameter is also generally regarded as a measure of the width of the saddle point of the potential energy surface, where the reactant molecules must pass as activated complexes. According to the thermodynamic data of the sorption isotherms, the sorption of ^{90}Sr(II) on GMZ bentonite can be concluded as being endothermic and spontaneous.

CONCLUSIONS

From the results of ^{90}Sr(II) sorption onto GMZ bentonite, the following conclusions can be drawn:

(1) The sorption of ^{90}Sr(II) onto GMZ bentonite is rather quick and the kinetic sorption can be described by the pseudo-second-order model very well.

(2) The sorption of ^{90}Sr(II) on GMZ bentonite is dependent on pH values and ionic strength at low pH, and is independent of ionic strength at high pH. It can be confirmed that the sorption mechanism of ^{90}Sr(II) is dominated by ion exchange or outer-sphere surface complexation at low pH values, and by inner-sphere surface complexation at high pH.

(3) The sorption of ^{90}Sr(II) on GMZ bentonite is influenced by foreign cation ions at low pH and is not influenced by foreign cation ions at high pH values, but the sorption is not influenced by foreign anion ions in the pH range of 3-12.

(4) The sorption of ^{90}Sr(II) is significantly influenced by HA, and the effect of HA on ^{90}Sr(II) sorption is dependent on pH. The sorption of ^{90}Sr(II) on GMZ bentonite is enhanced at low pH values but is reduced at high pH values.

(5) The thermodynamic data calculated from temperature dependent sorption isotherms suggests that the sorption reaction is a spontaneous and endothermic process.

(6) The good sorption of ^{90}Sr(II) on GMZ bentonite suggests that the bentonite from the Gaomiaozi Country (Inner Mongolia, China) is suitable as backfill material in a nuclear waste repository.

ACKNOWLEDGEMENT

Financial support from National Natural Science Foundation of China (21377132, 21307135), the special scientific research fund of public welfare profession (environmental protection) of China (201509074) and the Jiangsu Provincial Key Laboratory of Radiation Medicine and Protection and the Priority Academic Program Development of Jiangsu Higher Education Institutions are acknowledged. The great assistance from Dr. Xiaoli Tan is also acknowledged.

REFERENCES

1. X. L. Tan, X. M. Ren, C. L. Chen and X. K. Wang, *Trac-Trend. Anal. Chem.*, **61**, 107 (2014).
2. G. X. Zhao, J. X. Li, X. M. Ren, C. L. Chen and X. K. Wang, *Environ. Sci. Technol.*, **45**, 10454 (2011).
3. D. D. Shao, G. S. Hou, J. X. Li, T. Wen, X. M. Ren and X. K. Wang, *Chem. Eng. J.*, **255**, 604 (2014).
4. J. Xiao, L. P. Zhao W. Zhang, X. Liu and Y. T. Chen, *Korean J. Chem. Eng.*, **31**(2), 253 (2014).
5. H. Chen, D. D. Shao, J. X. Li and X. K. Wang, *Chem. Eng. J.*, **254**,

623 (2014).
6. Y. B. Sun, J. X. Li and X. K. Wang, *Geochim. Cosmochim. Ac.*, **140**, 621 (2014).
7. S. C. Tsai, S. Ouyang and C. N. Hsu, *Appl. Radiat. Isotopes.*, **54**, 209 (2001).
8. M. H. Al-Qunaibit, W. K. Mekhemer and A. A. Zaghloul, *J. Colloid Interface Sci.*, **283**, 316 (2005).
9. H. Omara, H. Aridab and A. Daifullah, *Appl. Clay. Sci.*, **44**, 21 (2009).
10. M. Majdana, S. Pikusa, A. Gajowiaka, D. Sternika and E. Ziębab, *J. Hazard. Mater.*, **184**, 662 (2010).
11. P. K. Verma, P. Pathak and P. K. Mohapatra, *Radiochim. Acta*, **102**, 401 (2014).
12. R. S. Singh and M. K. Mondal, *Korean J. Chem. Eng.*, **29**(12), 1782 (2012).
13. W. B. Jia and S. S. Lu, *J. Radioanal. Nucl. Chem.*, **299**, 1417 (2014).
14. D. Q. Pan, Q. H. Fan, P. Li, S. P. Liu and W. S. Wu, *Chem. Eng. J.*, **172**, 898 (2011).
15. J. X. Li, J. Hu, G. D. Sheng, G. X. Zhao and Q. Huang, *Colloids Surf., A.*, **349**, 195 (2009).
16. D. L. Zhao, S. H. Chen, S. B. Yang, X. Yang and S. T. Yang, *Chem. Eng. J.*, **166**, 1010 (2011).
17. S. W. Wang, Y. H. Dong, M. L. He, L. Chen and X. J. Yu, *Appl. Clay. Sci.*, **43**, 164 (2009).
18. Y. M. Liu and Z. R. Chen, *Acta. Mineral. Sin.*, **21**, 541 (2001).
19. B Ma, S Oh, W. S. Shin and S. J. Choi, *Desalination*, **276**, 336 (2011).
20. S. T. Yang, J. X. Li, Y. Lu, Y. X. Chen and X. K. Wang, *Appl. Radiat. Isotopes.*, **67**, 1600 (2009).
21. Z. Y. Tao, J. Zhang and J. J. Zhai, *Anal. Chim. Acta*, **395**, 199 (1999).
22. X. L. Tan, Q. H. Fan, X. K. Wang and B. Grambow, *Environ. Sci. Technol.*, **43**, 3115 (2009).
23. S. T. Yang, G. D. Sheng, X. L. Tan, J. Hu, J. Z. Du, G. Montavon and X. K. Wang, *Geochim. Cosmochim. Ac.*, **75**, 6520 (2011).
24. S. T. Yang, G. D. Sheng, G. Montavon, Z. Q. Guo, X. L. Tan, B. Grambow and X. K. Wang, *Geochim. Cosmochim. Ac.*, **121**, 84 (2013).
25. X. K. Wang, T. Rabung, H. Geckeis, P. J. Panak, R. Klenze and T. Fanghänel, *Radiochim. Acta*, **92**, 691 (2004).
26. Y. S. Ho and G. Mckay, *Process. Saf. Environ.*, **76**, 183 (1998).
27. M. K. Mondal, *Korean J. Chem. Eng.*, **27**(1), 144 (2010).
28. Q. H. Fan, D. D. Shao, W. S. Wu and X. K. Wang, *Chem. Eng. J.*, **150**, 188 (2009).
29. Ş. Kubilay, R. Gürkan, A. Savran and T. Şahan, *Adsorption*, **13**, 41 (2007).
30. A. Kowal-Fouchard, R. Drot, E. Simoni and J. J. Ehrhardt, *Environ. Sci. Technol.*, **38**, 1399 (2004).
31. T. Cole, G. Bidoglio, M. Soupioni, M. O'Gorman and N. Gibson, *Geochim. Cosmochim. Ac.*, **64**, 385 (2000).
32. A. Kayaa and A. H. Ören, *J. Hazard. Mater.*, **125**, 183 (2005).
33. R. Naseem and S. S. Tahir, *Water Res.*, **35**, 3982 (2001).
34. K. L. Mercer and J. E. Tobiason, *Environ. Sci. Technol.*, **42**, 3797 (2008).
35. Y. Zhao, Z. Y. Shao, C. L. Chen, J. Hu and H. L. Chen, *Appl. Clay. Sci.*, **87**, 1 (2014).
36. H. Chen, J. X. Li, S. W. Zhang, X. M. Ren, Y. B. Sun, T. Wen and X. K. Wang, *Radiochim. Acta*, **101**, 785 (2013).
37. G. D. Sheng, S. T. Yang, J. Sheng, J. Hu, X. L. Tan and X. K. Wang, *Environ. Sci. Technol.*, **45**, 7718 (2011).
38. E. Tertre, G. Berger, S. Castet, M. Loubet and E. Giffaut, *Geochim. Cosmochim. Ac.*, **69**, 4937 (2005).
39. S. W. Wang, J. Hu, J. X. Li and Y. H. Dong, *J. Hazard. Mater.*, **167**, 44 (2009).
40. F. Esmadi and J. Simm, *Colloids Surf., A.*, **104**, 265 (1995).
41. M. Y. Zeng, Y. S. Huang, S. W. Zhang, S. Qin, J. X. Li and J. Z. Xu, *RSC Adv.*, **4**, 5021 (2014).
42. L. Q. Tan, Y. L. Jin, J. Chen, X. C. Chen, J. Wu and L. D. Feng, *J. Radioanal. Nucl. Chem.*, **289**, 601 (2011).
43. T. H. Yoon, H. Moon, Y. J. Park and K. K. Park, *Environ. Sci. Technol.*, **28**, 2139 (1994).
44. Y. Takahashi, Y. Minai, S. Ambe, Y. Makide and F. Ambe, *Geochim. Cosmochim. Ac.*, **63**, 815 (1999).
45. G. Montavon, S. Markai, Y. Andrés and B. Grambow, *Environ. Sci. Technol.*, **36**, 3303 (2002).
46. I. Langmuir, *J. Am. Chem. Soc.*, **40**, 1361 (1918).
47. X. M. Ren, S. W. Wang, S. T. Yang and J. X. Li, *J. Radioanal. Nucl. Chem.*, **283**, 253 (2010).
48. Q. H. Fan, X. L. Tan, J. X. Li, X. K. Wang, W. S. Wu and G. Montavon, *Environ. Sci. Technol.*, **43**, 5776 (2009).
49. R. Donat, A. Akdogan, E. Erdem and H. Cetisli, *J. Colloid Interface Sci.*, **286**, 43 (2005).
50. A. Özcan, E. M. Öncü and A. S. Özca, *Colloids Surf., A.*, **277**, 90 (2006).
51. S. S. Tahir and N. Rauf, *J. Chem. Thermodyn.*, **35**, 2003 (2003).
52. G. D. Sheng, J. X. Li, D. D. Shao, J. Hu, C. L. Chen, Y. X. Chen and X. K. Wang, *J. Hazard. Mater.*, **178**, 333 (2010).
53. H. Genç-Fuhrman, J. C. Tjell and D. Mcconchie, *Environ. Sci. Technol.*, **38**, 2428 (2004).